Journal of Hazardous Materials 183 (2010) 641–647

Contents lists available at ScienceDirect

Journal of Hazardous Materials

journal homepage: www.elsevier.com/locate/jhazmat

# Treatment of VOCs with molecular sieve catalysts in regenerative catalytic oxidizer

Shih-Wei Huang [a,*], Jie-Chung Lou [b], Yung-Chang Lin [c]

[a] Department of Earth and Environmental Sciences, National Chung Cheng University,168 University Road, Minhsiung Township, Chiayi County 62102, Taiwan, ROC
[b] Institute of Environmental Engineering, National Sun Yat-Sen University, Kaohsiung, Taiwan, ROC
[c] Department of Electrical Engineering, Cheng Shiu University, Kaohsiung County, Taiwan, ROC

ARTICLE INFO

*Article history:*
Received 29 April 2010
Received in revised form 26 June 2010
Accepted 18 July 2010
Available online 24 July 2010

*Keywords:*
Molecular sieve
Cu catalyst
Regenerative catalytic oxidizer
Thermal recovery efficiency

ABSTRACT

This work prepares molecular sieve catalysts with various metal species and various metal weight loadings by impregnation, and then screens them in a catalytic combustion system. The current study further investigates the molecular sieve catalyst in an RCO system after it performed well in combustion efficiency. This work tests its performances in terms of $CO_2$ yield, pressure drop, the difference between temperatures of the inlet and outlet gases ($T_d$), and thermal recovery efficiency (TRE), with various operational conditions. Experimental results demonstrate that the 10 wt% Cu/(MS) catalyst was the most active because it has the greatest combustion efficiency to treat volatile organic compounds (VOCs) than Co/(MS) catalysts and Mn/(MS) catalysts. The 10 wt% Cu/(MS) catalyst used in an RCO system reaches over 95% $CO_2$ yields under the heating zone temperature ($T_{set}$) = 400 °C, gas velocity ($U_g$) = 0.37 m/s, isopropyl alcohol (IPA) concentration = 200–400 ppm conditions. Moreover, the RCO system performed well in economic efficiency with the RCO with in terms of TRE, $T_d$ and pressure drop. The TRE ranged from 90.4% to 94.6% and $T_d$ ranged from 14.0 to 34.2 °C under various conditions at $T_{set}$ = 300–450 °C. Finally, the results of the stability test demonstrated that the catalyst was very stable at various $U_g$ values and various $T_{set}$ values.



## 1. Introduction

Volatile organic compounds (VOCs) are recognized as major contributors to air pollution owing to their detrimental effect on human health and the environment. The health effects of VOCs include immune effects, cellular effects, cardiovascular effects, neurogenic and sensory effects, and some respiratory effects [1]. The main environmental concern of VOCs involves the formation of photochemical smog. In the presence of nitrogen oxides, VOCs are the precursors to the formation of ground level ozone [2]. VOCs are produced and emitted by natural and anthropogenic activity. Anthropogenic VOC emissions typically come from either mobile or stationary sources [3]. According to data from the United State Environmental Protection Agency (USEPA), the main source of VOCs emissions by source sector were; solvent use, on road vehicles, nonroad equipment, and industry processes. In all, they exceeded million tons in United State in 2005 [4]. A concerted effort will be needed to place limits on VOC emissions, and cost-effective, efficient techniques to treat VOCs will have to be developed.

Many techniques can be used to remove VOCs, including absorption, adsorption, thermal combustion, catalytic oxidation, regenerative thermal oxidizer (RTO), and regenerative catalytic oxidizer (RCO) [5–7]. Among them, the RCO technique combines catalytic oxidation and a thermal recovery system, obtaining higher treatment efficiency, lower operational temperature, lower fuel cost, and the formation of fewer harmful by-products, as a more energy-efficient method for eliminating VOCs [8–10]. Chou et al. [9] used the RCO to treat methyl ethyl ketone and toluene by providing a VOC removal efficiency of 98% for MEK and 95% for toluene. Strots et al. [10] found that the retrofitting of regenerative thermal oxidizers (RTO) into catalytic units provided 30–70% energy savings, a reduction in the pressure drop, or a 15–25% increase in the flow rate.

Currently, the catalysts used in abating VOC emission are normally divided into noble metal catalysts and metal oxide catalysts. Noble metal catalysts typically exhibit higher activities than other metal oxide based catalysts, but they are limited by higher cost and sensitivity of the noble metal based catalysts to poisoning [11]. Metal oxide based catalysts are much cheaper, allowing a higher catalyst load, leading to higher active surface area in the metal oxide based catalyst. It also lowers the catalytic sensitivity to nonselective poisoning [12,13]. Thus, many researchers have worked to gain higher activity and resistance to poisoning of metal

* Corresponding author. Fax: +886 5 2720807.
*E-mail addresses:* envheroson@hotmail.com, envhero@yahoo.com.tw (S.-W. Huang).

0304-3894/$ – see front matter © 2010 Elsevier B.V. All rights reserved.
doi:10.1016/j.jhazmat.2010.07.073

**Nomenclature**

| | |
|---|---|
| Conc. | experimental influent VOC concentration (ppm) |
| $d_p$ | average equivalent diameter of the solid particles (cm) |
| GHSV | gas hourly space velocity ($h^{-1}$) |
| $N$ | number carbon atoms in each VOC molecule |
| $n$ | number of the solid particle in the container with a volume of 10 L |
| $P_{CO_2}$ | concentration of production of $CO_2$ (ppm) |
| $S_h$ | the specific heat of solid particle (J/kg K) |
| $S_t$ | valve shifting time (min) |
| $T_c$ | thermal capacity of solid particles in the chamber (J/K) |
| $T_d$ | temperature difference between inlet and outlet gases of RCO system (°C) |
| $T_i$ | influent gas temperature to the bed (°C) |
| $T_{max}$ | maximum gas temperature in the bed (°C) |
| $T_o$ | outlet gas temperature from the bed (°C) |
| TRE | thermal recovery efficiency of RCO system (%) |
| $T_{set}$ | reaction set temperature of RCO system (°C) |
| $U_g$ | gas velocity (m/sec) |
| $V$ | volume of chamber ($cm^3$) |
| $W$ | weight of the solid particles in the container with a volume of 10 L (g) |
| $Z$ | penetration depth (m) |
| $\varepsilon$ | bed voidage (%) |
| $\rho_s$ | density of the solid particle ($g/cm^3$) |

oxide catalysts to reduce the cost of VOC removal. In this work, the RCO system includes metal oxide catalysts and reports on the metal oxide species, metal loading, the type of support, and the preparation method that affects the removal efficiency of VOCs [12–16]. Among metal oxide catalysts, researchers have reported copper catalysts, manganese catalysts, and cobalt catalysts to be the active metal oxides among metal oxide catalysts for VOC combustion. Larsson and Andersson noted the excellent performance in catalytic combustion of CO, ethyl acetate, and ethanol over $CuOx/Al_2O_3$ [12]. Tseng and Chu [17] reported that metal oxide catalysts ($MnO/Fe_2O_3$) performed well in the catalytic oxidation of styrene. Cobalt catalysts prepared with various Co contents to treat benzene, exhibited different efficiencies with Co wt% [18]. Among the above literatures, copper, manganese, and cobalt may be the appropriate active metal oxides among the metal oxide catalysts for VOC combustion, and the present study selects them for investigation.

The key aspects in an RCO system, including packing catalysts and operational parameters, are confidential and the literature provides only limited information. This study employs a molecular sieve as a carrier, supported various Cu, Mn, and Co metals with different metal loadings by impregnation, and screens their performances in the combustion of isopropyl alcohol (IPA) in a catalytic incineration system to identify optimal metal loading and metal oxide species. This work further investigates optimal metal loading and metal oxide species on the molecular sieve catalyst in an RCO system. This research tested its performances in terms of $CO_2$ yield, thermal recovery efficiency (TRE), and temperature difference between inlet and outlet gases ($T_d$) and pressure drop by varying gas velocity ($U_g$), inlet IPA concentration, shift time ($S_t$), and reaction set temperature ($T_{set}$). Finally, the current investigation studied the catalyst stability in an RCO and used SEM/EDS to observe the surface of catalyst.

## 2. Materials and methods

### 2.1. Preparation of catalyst

In this study, molecular sieves were employed as supports for the catalysts. Various Cu, Mn, and Co metals with various metal loadings were supported on molecular sieves to evaluate the efficiency of catalytic combustion.

First, metal oxide catalysts supported on molecular sieves with various metal loading were prepared by the incipient wetness impregnation method, using various concentrations of aqueous Cu $(NO_3)_2{\cdot}3H_2O$, Co $(NO_3)_2{\cdot}6H_2O$ and Mn $(NO_3)_2{\cdot}6H_2O$. The volume of the impregnation solution was equal to the pore volume of the support, and the volume ratio of impregnation solution to support was 33:67. The impregnated samples were heated to 80 °C on a heating board for 30 min and dried in an oven with a temperature of 105 °C for 48 h. Subsequently, the dried samples were calcined with airflow (1 L/min) at 600 °C for 4 h in a furnace to obtain the final form of supported catalysts. The various metal we obtained (Cu, Mn, and Co), supported on molecular sieves with 5 wt% or 10 wt% metal loading were denoted as 5 wt% Cu/(MS), 5 wt% Mn/(MS), 5 wt% Co/(MS), 10 wt% Cu/(MS), 10 wt% Mn/(MS), 10 wt% Co/(MS), respectively.

### 2.2. Experimental instruments

Catalyst screening combustions of IPA on all molecular sieve catalysts were carried out at atmospheric pressure in a catalytic reactor system (Fig. 1). Then the molecular sieve catalysts that exhibited the highest activity were used in the RCO system (Fig. 2) to investigate combustion efficiency and economic performance. Fig. 1 depicts the catalytic combustion system. IPA, nitrogen ($N_2$) and oxygen ($O_2$) were used in the gaseous IPA manipulating system; the flow rates and concentrations of these three gases were controlled by flow meters. Then the gases were completely mixed in a mixer before being sent to the catalytic reactor. The catalytic reactor was a fixed-bed quartz tubular reactor with 30 mm diameter and 40 cm length, placed inside an electric heating oven equipped with a proportional integral derivative (PID) controller. The catalysts were supported by quartz wool in the middle of the quartz tube, and a K-type thermocouple positioned in the middle of the catalyst chamber was used to measure the accurate reaction temperature.

Fig. 2 presents the diagram of the experimental RCO system. The RCO contains two beds with packing media, and each bed has four chambers with dimensions 15 cm length × 15 cm width × 25 cm height. The chambers closest to the heating zone (A1 and B1) were completely filled with catalysts, and the others were filled

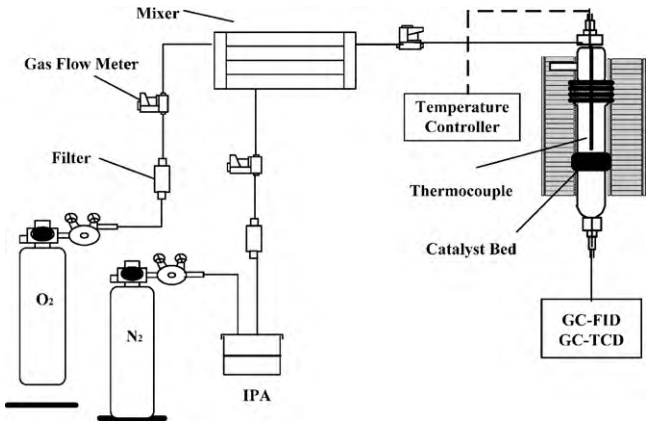


**Fig. 1.** Experimental instrument for catalytic incineration system.

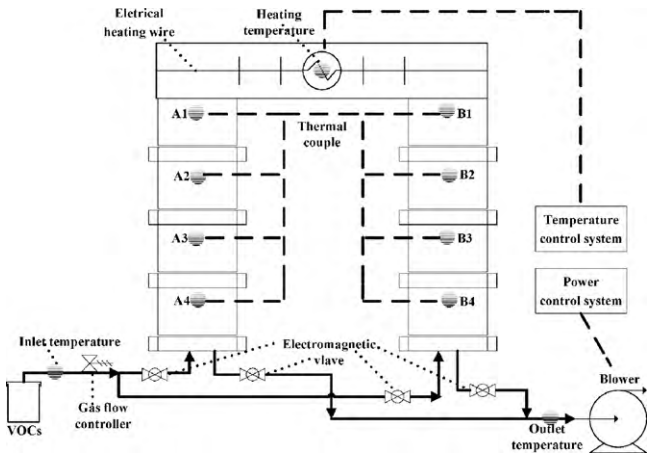


**Fig. 2.** Diagram of the experimental RCO system.

with regenerative gravel particles. The beds were constructed from stainless steel and the outer walls of both beds were wrapped in ceramic fiber for thermal insulation. The RCO was equipped with two pressure gauges to measure the pressure drop, four electromagnetic valves to shift the influent air stream, and one blower with a normal capacity of 2.5 $m^3$/min. The RCO was electrically heated by the PID controller, and the temperature-controlled sensor was positioned in the heating temperature zone. Moreover, the RCO was also equipped with eight thermal couples for eight chambers to understand the variation of beds' temperature, and two for the inlet gas and the outlet exhaust to measure $T_d$ values.

Finally, in both the catalytic reactor system and the RCO system, the VOC concentrations of inlet and outlet gases were analyzed using a gas chromatograph, GC-14A model (Shimadzu) with a flame ionization detector (GC-FID), and the concentrations of $CO_2$ and CO in the effluent gas were determined using a GC-14A with a thermal conductivity detector (GC-TCD). The yields of $CO_2$ were calculated using the following Eq. (1).

$$\text{Yields of } CO_2 = \frac{P_{CO_2}}{(\text{Conc.} \times N)} \times 100\% \quad (1)$$

where $P_{CO_2}$ (ppm) denotes the concentration of production of $CO_2$; Conc. (ppm) is the inlet VOCs concentration; $N$ is the number carbon atoms in each VOC molecule.

### 2.3. Properties of catalytic support and regenerative gravel

Table 1 shows the properties of catalytic support and regenerative gravel. The procedures and methods characterizing catalytic support and regenerative gravel are presented as follows: The solid particles were saturated in water, and moved to a container with a volume of 10 L. The container was filled with water after placing the materials. Bed voidage ($\varepsilon$) was achieved by dividing the water in the container into the volume of the container (10 L). We can gain an average equivalent diameter of the solid particles by Eq. (2) and gain the density of solid particle by Eq. (3).

$$d_p = \left[\frac{6(1-\varepsilon)(10,000)}{(n\pi)}\right]^{1/3} \quad (2)$$

$$\rho_s = \frac{W}{[10,000(1-\varepsilon)]} \quad (3)$$

where $d_p$ (cm) is the average equivalent diameter of the solid particle; $n$ is the number of the solid particles in the container with a volume of 10 L; $\rho_s$ (g/$cm^3$) is the density of the solid particle; $W$ (g) is the weight of the solid particles in the container with a volume of 10 L. The data for the specific heat of molecular sieve and gravel were obtained from the manufacturers (Hi-lyte, Taiwan) and Perry's chemical engineers' handbook, respectively [19].

**Table 1**
Properties of catalytic support and regenerative gravel.

| Material | Molecular sieve | Gravel |
|---|---|---|
| Type | 4A | Cement manufacture |
| Shape | Sphericity | Random |
| Bed voidage ($\varepsilon$,%) | 33 | 52 |
| Size (cm) | 0.31 | 1.12 |
| Density ($\rho_s$, g/$cm^3$) | 0.75 | 2.31 |
| Specific heat($S_h$, J/kg K) | 920 | 840 |

### 2.4. Screening catalytic activity in catalytic combustion system

The activity tests of various metal species and metal loading catalysts were examined in the temperature range of 100–500 °C, with an inlet IPA concentration of 1000 ppm, an oxygen concentration of 21%, and a space velocity of 12,000 $h^{-1}$. The reaction temperature heated in steps of 50 °C to 500 °C at a heating rate of 3 °C/min, and the temperature was held for 10 min to ensure the steady-state condition in each step. Then the exhausts were sampled and analyzed to calculate the $CO_2$ yield. The $CO_2$ yields obtained using various catalysts were compared to identify the most effective catalyst, which was used in the RCO system for further investigation.

### 2.5. RCO system test

In the RCO approach, inert regenerative gravels and catalysts are applied to pre-heat the inlet air stream and to cool the outlet air stream, reducing the wasted energy. The beds' temperatures of the RCO are balanced in a sequence of cyclic operations, which vary the direction of the air stream through a fixed $S_t$ value. The gas temperatures in the bed and outlet stream were steady with time for a specified set of operation conditions and then a VOC concentration setting was sent to the air stream to start the catalytic combustion. During the reaction period of two hours, the exhausts were sampled and analyzed twelve times to evaluate the combustion efficiency, and the gas temperature variation in the regenerative beds, TRE, and the $T_d$ and pressure drop were recorded to elucidate the economic efficiency. We can gain the TRE of a RCO by Eq. (4).

$$\text{TRE} = \frac{[T_{max} - T_o]}{[T_{max} - T_i]} \times 100\% \quad (4)$$

where $T_{max}$ is the maximum gas temperature in the beds (°C); $T_i$ is the temperature of the influent gas to the bed (°C), and $T_o$ is the temperature of the outlet gas from the bed (°C).

Moreover, the combustion efficiency ($CO_2$ yield) and economic efficiency (TRE, $T_d$ and pressure drop) of the RCO with various operational parameters, including inlet VOC concentration, $T_{set}$, and $U_g$, were discussed to identify the optimal parameters. Finally, the catalyst stability was analyzed.

## 3. Results and discussion

### 3.1. Screening catalytic activity in catalytic combustion system

Various metal species (Cu, Mn, Co) and various metal loadings (5 wt%, 10 wt %) were supported on molecular sieves by impregnation. Fig. 3 plots the $CO_2$ yield of IPA treated with various catalysts as a temperature function. For a comparison of catalytic efficiency at a reaction temperature of 500 °C, the $CO_2$ yields decreased, in the following order Mn/(MS), Cu/(MS), Co/(MS) at 5 wt% metal loading, while at 10 wt% metal loading, they decreased, in the following

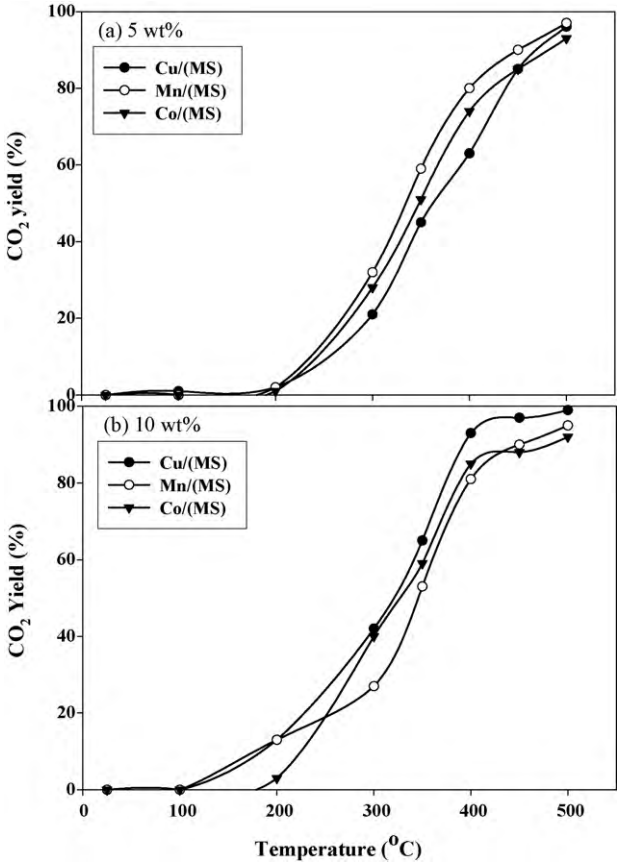


**Fig. 3.** $CO_2$ yield for treating IPA on various catalysts as function of temperature (a) 5% weight loading; (b) 10% weight loading. (Inlet IPA Conc. = 1000 ppm, GHSV = 12,000 $h^{-1}$, $O_2$ = 21%).

order Cu/(MS), Mn/(MS), Co/(MS) (Fig. 3a and b). In the case of Mn and Co, loading increased from 5 wt% to 10 wt%, and the effect of metal loading was slight. The $CO_2$ yields of 5 wt% Mn/(MS) and 10 wt% Mn/(MS) were 89.5% and 90.4% and those of 5 wt% Co/(MS) and 10 wt% Co/(MS) were 85.8% and 88.0%, respectively, at a reaction temperature of 450 °C. The result indicated that the 5 wt% Mn and Co metal supported on molecular sieves were nearly saturated. In the case of 5 wt% Cu/(MS) and 10 wt% Cu/(MS) catalysts, the $CO_2$ yields were 21.2% and 42.9% at a reaction temperature of 300 °C, and 85.4% and 97.2%, respectively, at a reaction temperature of 450 °C. In the case of 5–10 wt%, the $CO_2$ yields significantly increased with Cu loading. The results demonstrated that the effect of metal loading depended on individual active metals, even on the same catalytic supports. Table 2 shows the temperature required for 50% $CO_2$ ($T_{50}$) and 95% $CO_2$ ($T_{95}$) yields when IPA was treated with various catalysts. As seen in Table 2, the lowest temperatures $T_{50}$ and $T_{95}$, 315 °C and 420 °C, were recorded with the 10 wt% Cu/(MS) catalyst, and the results agreed with previous studies that the Cu based catalyst exhibited the lowest combustion temperatures among the various

**Table 2**
$T_{50}$ and $T_{95}$ of various catalysts.

| Metal species | Metal loading | $T_{50}$ (°C) | $T_{95}$ (°C) |
|---|---|---|---|
| Cu | 5 wt% | 365 | 495 |
| | 10 wt% | 315 | 420 |
| Mn | 5 wt% | 320 | 490 |
| | 10 wt% | 340 | 500 |
| Co | 5 wt% | 350 | – |
| | 10 wt% | 320 | – |

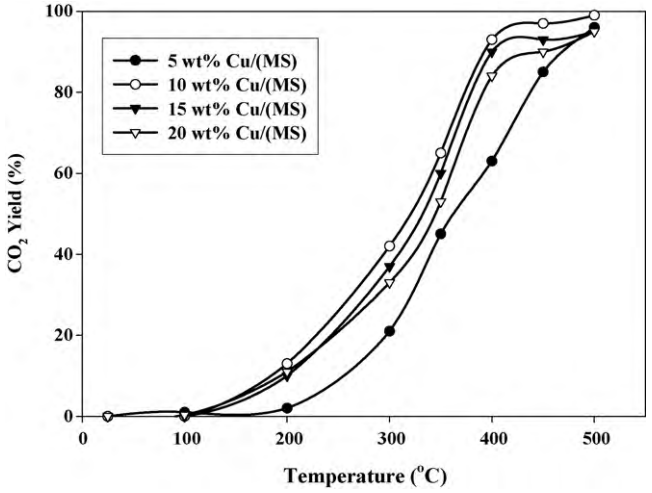


**Fig. 4.** $CO_2$ yield for treating IPA under different weight loadings of Cu as a function of temperature (Inlet IPA Conc. = 1000 ppm, GHSV = 12,000 $h^{-1}$, $O_2$ = 21%).

metal based catalysts (Cu, Co, Fe, Mn, Ni, etc.) for VOC combustion [13,14]. The difference in activity may be due to the difference in catalyst adsorption of VOCs and $O_2$; and the differences in BET surface area had no significant effect on combustion efficiency [20].

Given that 10 wt% Cu/(MS) catalyst was preferred for the combustion of IPA, we examined the effect of altering the Cu loading of this catalyst on catalytic performance (Fig. 4). As CuO is the active species in the Cu/(MS) catalyst, we expected that increasing the quantity of CuO with good dispersion would increase catalytic activity, thereby increasing the combustion efficiency of IPA [13,20]. Fig. 4 indicates that the $CO_2$ yields decreased, following the order 10 wt%/(MS), 15 wt%/(MS), 20 wt%/(MS), and 5 wt%/(MS), and the optimal Cu loading was about 10 wt%. Wang [13] and Kim [14] reported that the optimal Cu loading could be attributed to the good dispersion of CuO surface phase. Lower loading of Cu may lead to insufficient active sites, and higher loading may lead to larger CuO crystals, with few active sites, thereby reducing combustion efficiency. Based on the results of Fig. 4, the 10 wt% Cu/(MS) catalyst was selected for further investigation in the following RCO operations.

### 3.2. Test of RCO

#### 3.2.1. Combustion efficiency with various operational parameters

Wang et al. [20] found that increasing gas velocity reduced conversion when $CuO/CeO_2$ catalyst was used to treat the toluene. García et al. [21] treated naphthalene with $CeO_2$, and found that a higher temperature required for complete oxidation of naphthalene increased with the gas velocity. Wang and Lin [22] stated that a higher reaction temperature is necessary at higher toluene concentrations. Previous studies have demonstrated that inlet gas velocity and inlet VOC concentrations may affect catalytic combustion efficiency, and the following RCO experiments therefore find out the optimal $U_g$ values and inlet VOC concentrations. Fig. 5 plots $CO_2$ yields after treating IPA with various $U_g$ values and inlet VOC concentrations as various $T_{set}$ values. At $T_{set}$ = 300 °C, the range of $CO_2$ yields for treating IPA were from 54% to 73%. However, as the $T_{set}$ increased to 450 °C, the $CO_2$ yields for IPA were all up to 95%. Therefore, the $CO_2$ yield increased obviously with temperature.

Moreover, results also demonstrate that the $CO_2$ yield decreased with the VOC inlet concentration at the range of $T_{set}$ = 300 °C to $T_{set}$ = 350 °C, probably because of an adsorbed massive inlet VOC concentration on the catalyst surface active sites, saturating the contact area between the reactants and the catalyst [20]. Although

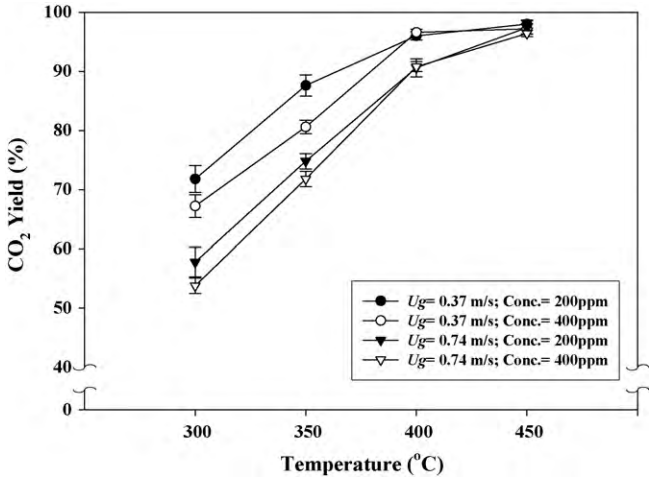


**Fig. 5.** $CO_2$ yield for treating IPA on various $U_g$ and inlet concentration values under various RCO $T_{set}$ values.

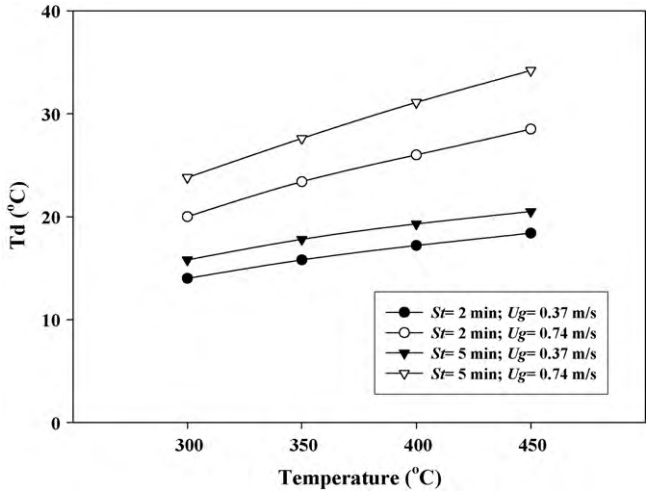


**Fig. 7.** $T_d$ for various $U_g$ and $S_t$ values under various RCO $T_{set}$ values.

the catalytic oxidation with a higher inlet VOC concentration releases more thermal energy, increasing the catalytic bed temperatures (A1 and B1 chambers) in the RCO system, the effects of inlet VOC concentrations on the catalysts evaluated here were still strong even when catalytic bed temperatures increased. However, the effect of inlet VOC concentrations was slight as the $T_{set}$ increased to $T_{set}$ = 400 °C or $T_{set}$ = 450 °C, especially in IPA oxidization.

Findings for the effect of $U_g$ show that the $CO_2$ yield increased obviously as the $U_g$ declined at the range of $T_{set}$ = 300–400 °C, and the effect was more obvious in lower $T_{set}$ values. For example, at $T_{set}$ = 300 °C and inlet IPA concentration = 200 ppm, the difference of $CO_2$ yield between $U_g$ of 0.37 m/s and 0.74 m/s was about 19% higher than 5% obtained at $T_{set}$ = 400 °C. Therefore, the effect of $U_g$ was not important in high reaction temperature and high $CO_2$ yield.

*3.2.2. Economic efficiency with various operational parameters*

*3.2.2.1. Pressure drop.* Fig. 6 plots the pressure drop of the RCO for various $U_g$ values and $S_t$ values at various $T_{set}$. At $U_g$ = 0.37 m/s and 0.74 m/s, the RCO system showed that the pressure drop ranged from 218 mm $H_2O$ to 254 mm $H_2O$ and 560 mm $H_2O$ to 655 mm $H_2O$, respectively. At the same $T_{set}$ values, pressure drop values attained under $U_g$ = 0.74 m/s were nearly greater than 2.5 times of those under $U_g$ = 0.37 m/s. Therefore, Fig. 5 demonstrates that the pressure drop increased with the $U_g$ and $T_{set}$ values, and the effect of the $U_g$ was especially marked. Moreover, the $S_t$ of 2 min increased to 5 min, and the pressure drops hardly varied. Therefore, the effect of $S_t$ value to pressure drop was negligible.

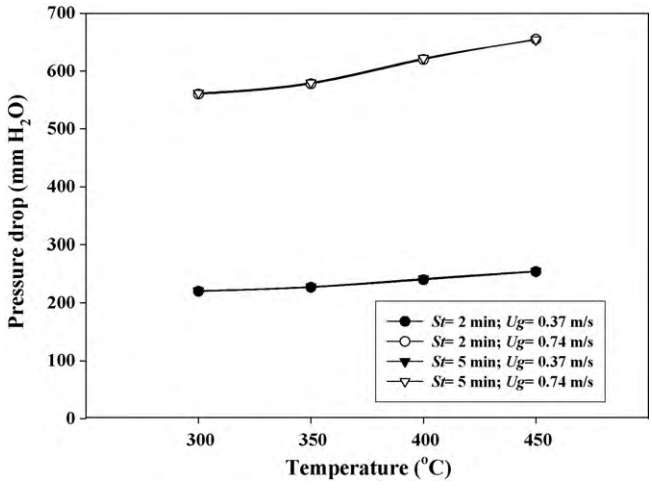


**Fig. 6.** Pressure drops for various $U_g$ and $S_t$ values under various RCO $T_{set}$ values.

*3.2.2.2. $T_d$.* The $T_d$ is important in estimating the lost thermal energy in RCO. Fig. 7 plots the $T_d$ values for various $U_g$ values and $S_t$ values as various $T_{set}$ in the RCO. The $T_d$ of the RCO ranged from 14.0 °C to 34.2 °C at $T_{set}$ = 300–450 °C, and it performed 17.2 °C and 19.3 °C under the $T_{set}$ = 400 °C and the $U_g$ = 0.37 m/s condition. Moreover, at fixed $S_t$ = 2 min conditions, the $T_d$ ranged from 14.0 °C to 18.4 °C and 20.0 °C to 28.5 °C under the $U_g$ = 0.37 m/s and 0.74 m/s conditions, respectively. At fixed $U_g$ = 0.37 conditions, the $T_d$ values under $S_t$ = 2 min were about 2 °C greater than those under $S_t$ = 5 min. Therefore, the above results demonstrate that $T_d$ increased with the $U_g$, $S_t$, and $T_{set}$ values.

*3.2.2.3. TRE.* Table 3 shows the TRE of the RCO under various operating conditions. From the table, the TRE range in an RCO system was from 90.4% to 94.6% under various operating conditions, and it performed 94.2% to 94.8% under the $T_{set}$ = 400 °C and $U_g$ = 0.37 m/s condition. Therefore, the RCO performed excellently in TRE. Moreover, Table 3 also demonstrates that TRE decreased as $U_g$ increased at fixed $S_t$ and $T_{set}$ values; TRE increased with $T_{set}$ at a fixed $S_t$ and $U_g$ values; and TRE decreased as $S_t$ of 2 min increased to $S_t$ of 5 min at fixed $T_{set}$ and $U_g$ values. The results reveal that $U_g$, $T_{set}$, and $S_t$ showed various significant effects on TRE and the effect of the $U_g$ was especially obvious.

The RCO of the 10 wt% Cu/(MS) catalyst performed excellently in TRE and $T_d$, probably because the specific heat of regenerative material-gravel and the catalyst support-molecular sieve are high. The thermal capacities of the gravel in the six regenerative chambers and the molecular sieve in the two catalyst chambers can be defined as Eq. (5).

$$T_c = S_h \times \rho_s \times (1 - \varepsilon) \times V \times 10^{-3} \quad (5)$$

where $T_c$ (J/K) is the thermal capacity of solid particles in the chamber; $S_h$ (J/kg K) is the specific heat; $V$ (cm$^3$) is the volume of chamber.

The $T_c$ of gravels in six regenerative chambers and the $T_c$ of molecular sieves in two catalyst chambers are 31,434 and 5201 (J/K), respectively. Accordingly, the RCO of the 10 wt% Cu/(MS) catalyst absorbs greater heat that it circulates and uses efficiently.

**Table 3**
TRE of the RCO with 10 wt% Cu/(MS) catalyst at different operation conditions.

| $S_t$ (min) | $U_g$ (m/s) | $T_{set}$ (°C) | $T_{A1}$ (°C) | $T_{B1}$ (°C) | $T_i$ (°C) | $T_o$ (°C) | TRE (%) |
|---|---|---|---|---|---|---|---|
| 2 | 0.37 | 300 | 242.1 | 250.0 | 26.1 | 40.1 | 93.7 |
| 2 | 0.74 | 300 | 247.8 | 257.0 | 25.4 | 45.4 | 91.4 |
| 2 | 0.37 | 350 | 287.1 | 290.3 | 25.0 | 40.8 | 94.0 |
| 2 | 0.74 | 350 | 292.1 | 303.4 | 25.5 | 48.9 | 91.6 |
| 2 | 0.37 | 400 | 320.1 | 320.8 | 24.9 | 42.1 | 94.2 |
| 2 | 0.74 | 400 | 327.0 | 334.6 | 25.5 | 51.5 | 91.6 |
| 2 | 0.37 | 450 | 360.2 | 365.4 | 24.8 | 43.2 | 94.6 |
| 2 | 0.74 | 450 | 367.8 | 375.8 | 26.0 | 54.5 | 91.8 |
| 5 | 0.37 | 300 | 243.4 | 262.3 | 25.4 | 41.2 | 93.3 |
| 5 | 0.74 | 300 | 248.4 | 273.2 | 26.0 | 49.8 | 90.4 |
| 5 | 0.37 | 350 | 288.0 | 304.1 | 25.8 | 43.6 | 93.6 |
| 5 | 0.74 | 350 | 293.0 | 317.4 | 26.1 | 53.7 | 90.5 |
| 5 | 0.37 | 400 | 322.4 | 335.3 | 26.0 | 45.3 | 93.8 |
| 5 | 0.74 | 400 | 328.3 | 351.8 | 25.5 | 56.6 | 90.5 |
| 5 | 0.37 | 450 | 364.4 | 382.1 | 26.0 | 46.5 | 94.2 |
| 5 | 0.74 | 450 | 370.1 | 394.3 | 25.8 | 60.0 | 90.7 |

### 3.2.3. Gas temperature variation in RCO beds

Fig. 8 presents steady-state gas temperature profiles in range with various $U_g$ values, $T_{set}$ values. In the figure, $Z$ = 0 m refers to the inlet gas; $Z$ = 0.125 m, 0.375 m, 0.625 m, 0.875 m, 1.125 m, 1.375 m, 1.625 m, 1.875 m refer to the center of A4, A3, A2, A1, B1, B2, B3, B4 chambers, respectively; $Z$ = 1 m refers to the heating zone, and $Z$ = 2 m refers to exhaust gas.

Fig. 8 demonstrates that all the chamber temperatures increased with $U_g$ values. Although, the catalyst chamber temperatures obviously increased with $U_g$ values, but the $CO_2$ yields still decreased significantly in the above results of $U_g$ values. Therefore, the effect of $U_g$ on $CO_2$ yield in an RCO system is marked. From Fig. 8, temperature differences in the middle sections of the beds ($Z$ = 0.125–0.875 m and 1.125–1.875 m) were smaller than those in the bottom ($Z$ = 0–0.125 m and 1.875–2 m) and the top of the beds ($Z$ = 0.875–1.0 m and 1.0–1.125 m). Temperature differences in the bottom of the beds were 148 °C and 122 °C under $U_g$ = 0.74 m/s and the $T_{set}$ = 450 °C- condition was greater than the temperature differences under the lower $U_g$ or lower $T_{set}$ condition. Accordingly, the temperature gradients in the bed entrance and exit declined as either $U_g$ or $T_{set}$ values fell. In the middle sections of beds, the temperature differences were 197 °C and 192 °C under $U_g$ = 0.74 m/s, the $T_{set}$ = 450 °C condition were greater than those temperature differences under the lower $T_{set}$ condition, but less than those temperature differences under the lower $U_g$ condition. Therefore, the temperature gradients in the middle sections of the beds increased with $T_{set}$ but declined as $U_g$ increased. Moreover, the temperature gradients in the top of the beds showed a similar tendency to those in the middle sections of the beds.

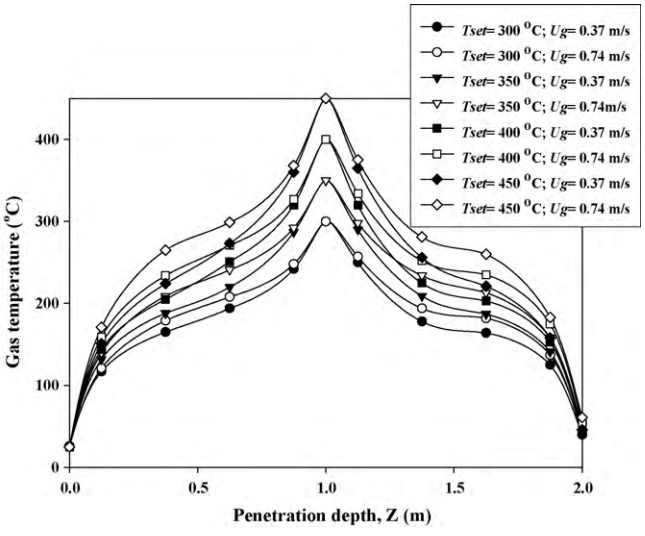


**Fig. 8.** Gas temperature profiles in the beds with different $T_{set}$ and $U_g$ values.

## 3.3. Stability of catalyst

Fig. 9 plots the catalytic oxidation of IPA with increasing $T_{set}$ under various $U_g$ values in a 96 h period test. Under the $U_g$ = 0.37 m/s condition, the $CO_2$ yield of IPA maintained from 72% to 74% at $T_{set}$ = 300 °C, from 82% to 86% at $T_{set}$ = 350 °C, and from 95% to 98% at $T_{set}$ = 400 °C and 450 °C, and the $CO_2$ yields of IPA under the $U_g$ = 0.74 m/s condition were also stable throughout the stability test. Therefore, the results demonstrate that the RCO of the 10 wt% Cu/(MS) catalyst exhibited excellent stability at various $T_{set}$ values and $U_g$ values.

## 3.4. SEM/EDS test

In this work, SEM (JEOL, JSM-6400) was used to observe the surface of the catalyst, and verify its alloy composition. Fig. 10 displays the SEM images of the 10 wt% Cu/(MS) catalyst. From the SEM image, the 10 wt% Cu/(MS) catalyst shows a morphology consisting of particle conglomerates and the particle size was nearly 1.5–2 μm. The result of the EDS test (Table 4) demonstrates that the catalyst surface components were O, Mg, Al, Si, Fe, and Cu, of

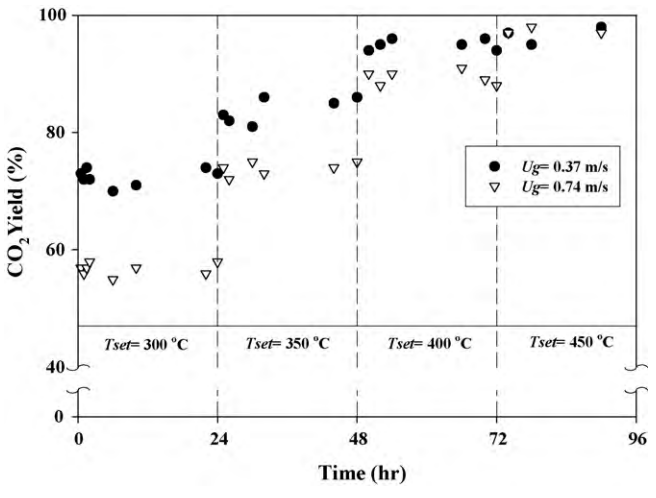


**Fig. 9.** $CO_2$ yield as reaction time under various $T_{set}$ values (inlet IPA Conc. = 200 ppm, $S_t$ = 2 min).

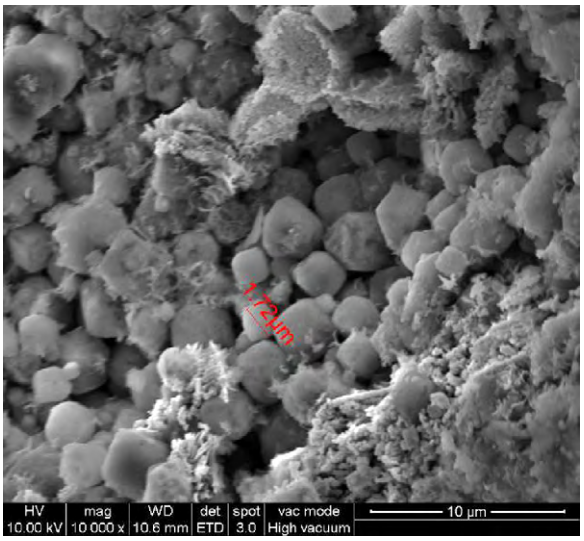


**Fig. 10.** The SEM images of 10 wt% Cu/(MS) catalyst.

**Table 4**
EDS test results of the 10 wt% Cu/(MS) catalyst.

| Element | Weight (%) | Atomic (%) |
|---|---|---|
| O | 39.41 | 61.47 |
| Mg | 1.48 | 1.52 |
| Al | 8.69 | 8.04 |
| Si | 18.30 | 16.27 |
| Fe | 1.56 | 0.70 |
| Cu | 30.56 | 12.00 |

which O, Mg, Al, Si, and Fe were the molecular sieve elements and Cu coated on the surface of molecular sieve was also observed.

## 4. Conclusions

The 10 wt% Cu/(MS) catalyst was selected to further investigate in RCO system because it has the lowest temperatures $T_{95}$, 420 °C, in the catalytic combustion system. The results of RCO operations with the 10 wt% Cu/(MS) catalyst demonstrated that combustion efficiency decreased as VOC concentration and $U_g$ values increased; the $T_d$ increased with the $U_g$, $S_t$, and $T_{set}$ values; TRE increased with $T_{set}$ values but decreased as $U_g$ and $S_t$ values increased. Over 95% of $CO_2$ yields were obtained at $T_{set}$ = 400 °C, $U_g$ = 0.37 m/s, and IPA concentration = 200–400 ppm, with the 10 wt% Cu/(MS) catalyst used in an RCO system. Moreover, the RCO system performed well in economic efficiency of the RCO in terms of TRE, $T_d$, and pressure drop. Finally, the results of the stability test demonstrated that the catalyst was very stable at various $U_g$ values and various $T_{set}$ values.

## Acknowledgment

The authors would like to thank the National Science Council of the Republic of China, Taiwan for financially supporting this research under Contract number NSC 95-2221-E-110-040.

## References

[1] L. Molhave, Organic compounds as indicators of air pollution, Indoor Air 13 (2003) 12–19.
[2] R. Beauchet, P. Magnoux, J. Mijoin, Catalytic oxidation of volatile organic compounds (VOCs) mixture (isopropanol/o-xylene) on zeolite catalysts, Catal. Today 124 (2007) 118–123.
[3] H.T. Nguyena, K.H. Kim, M.Y. Kim, Volatile organic compounds at an urban monitoring station in Korea, J. Hazard. Mater. 161 (2009) 163–174.
[4] United State Environmental Protection Agency, National Summary of VOC Emissions in 2005, http://www.epa.gov/air/emissions/voc.htm.
[5] M.S. Chou, C.M. Hei, Regenerative thermal oxidation of airborne *N*,*N*-dimethyl formamide and its associated nitrogen oxides formation characteristics, J. Air Waste Manage. Assoc. 57 (2007) 991–999.
[6] B.J. Park, G.S. Hwang, S.J. Haam, C.H. Lee, I.S. Ahn, K.J. Lee, Absorption of a volatile organic compound by a jet loop reactor with circulation of a surfactant solution: performance evaluation, J. Hazard. Mater. 153 (2008) 735–741.
[7] H. Zaitan, D. Bianchi, O. Achak, T. Chafik, A comparative study of the adsorption and desorption of *o*-xylene onto bentonite clay and alumina, J. Hazard. Mater. 153 (2008) 852–859.
[8] M. Amelio, P. Morrone, Numerical evaluation of the energetic performances of structured and random packed beds in regenerative thermal oxidizers, Appl. Therm. Eng. 27 (2007) 762–770.
[9] M.S. Chou, W.H. Cheng, W.S. Li, Performance characteristics of a regenerative catalytic oxidizer to treat VOC-contaminated air stream, J. Air Waste Manage. Assoc. 50 (2000) 2112–2119.
[10] V.O. Strots, G.A. Bunimovich, C.R. Roach, Y.S. Matros, Regenerative catalytic oxidizer technology for VOC control, React. Eng. Pollut. Prevent. (2000) 113–126.
[11] J. Lojewska, A. Kolodziej, J. Zak, J. Stoch, J. Pd/Pt promoted $Co_3O_4$ catalysts for VOCs combustion: preparation of active catalyst on metallic carrier, Catal. Today 105 (2005) 655–661.
[12] P.O. Larsson, A. Andersson, Oxides of copper, ceria promoted copper, manganese and copper manganese on $Al_2O_3$ for the incineration of CO, ethyl acetate and ethanol, Appl. Catal. B: Environ. 24 (2000) 175–192.
[13] C.H. Wang, $Al_2O_3$-supported transition-metal oxide catalysts for catalytic incineration of toluene, Chemosphere 55 (2004) 11–17.
[14] S.C. Kim, The catalytic oxidation of aromatic hydrocarbons over supported metal oxide, J. Hazard. Mater. 91 (2002) 285–299.
[15] A.Z. Abdullah, M.Z.A. Bakar, S. Bhatia, Combustion of chlorinated volatile organic compounds (VOCs) using bimetallic chromium-copper supported on modified H-ZSM-5 catalyst, J. Hazard. Mater. 129 (2006) 39–49.
[16] F. Wyrwalski, J.F. Lamonier, S. Siffert, A. Aboukais, Additional effects of cobalt precursor and zirconia support modifications for the design of efficient VOC oxidation catalysts, Appl. Catal. B: Environ. 70 (2007) 393–399.
[17] T.K. Tseng, H. Chu, The kinetics of catalytic incineration of styrene over a $MnO/Fe_2O_3$ catalyst, Sci. Total Environ. 275 (2001) 83–93.
[18] T. Ataloglou, J. Vakros, K. Bourikas, C. Fountzoula, C. Kordulis, A. Lycourghiotis, Influence of the preparation method on the structure–activity of cobalt oxide catalysts supported on alumina for complete benzene oxidation, Appl. Catal. B: Environ. 57 (2005) 299–312.
[19] R.H. Perry, D.W. Green, Perry's Chemical Engineers' Handbook, 7th ed., McGraw-Hill, New York, 1997.
[20] C.H. Wang, S.S. Lin, C.L. Chen, H.S. Weng, Performance of the supported copper oxide catalysts for the catalytic incineration of aromatic hydrocarbons, Chemosphere 64 (2006) 503–509.
[21] T. García, B. Solsona, S.H. Taylor, Naphthalene total oxidation over metal oxide catalysts, Appl. Catal. B: Environ. 66 (2006) 92–99.
[22] C.H. Wang, S.S. Lin, Preparing an active cerium oxide catalyst for the catalytic incineration of aromatic hydrocarbons, Appl. Catal. A: Gen. 268 (2004) 227–233.